Ocean Engineering 195 (2020) 106680

Contents lists available at ScienceDirect

Ocean Engineering

journal homepage: www.elsevier.com/locate/oceaneng

Experimental study on influence of excess pore water pressure and unloading ratio on unloading mechanical properties of marine sedimentary soft soils

Wei Huang [a,b], Kejun Wen [c,*], Dongyan Liu [a,b], Qian Dong [d], Junjie Li [a], Yang Li [c], Lin Li [e]

[a] School of Civil Engineering and Architecture, Chongqing University of Science and Technology, Chongqing, 401331, China
[b] Chongqing Key Laboratory of Energy Engineering Mechanics & Disaster Prevention and Mitigation, Chongqing, 401331, China
[c] Department of Civil and Environmental Engineering, Jackson State University, Jackson, MS, 39217, USA
[d] International Relations Office, Chongqing University of Science and Technology, Chongqing, 401331, China
[e] Department of Civil and Architectural Engineering, Tennessee State University, Nashville, TN, 37209, USA

ARTICLE INFO

Keywords:
Excess pore water pressure
Soft soil
Unloading mechanic
Stress path

ABSTRACT

The paper discussed the effects of pore water pressure and unloading ratio on the mechanical properties of soft soils. The Shenzhen marine sedimentary soft soils were selected in this study. The results revealed that the excess pore water pressures had significant weakening effects on the unloading strength of soft soils. Comparing with the unloading strength without excess pore water pressure, the reduction rate of unloading strengths at excess pore water pressure ranging from 20 to 60 kPa were found to be 3.4%–21.4% and 1.3%–19.2% for unloading ratio 0.0 and 0.5 respectively. Meanwhile, the excess pore water pressures had greater impact to cohesion than to internal friction angle. The unloading failure modes of soft soils are sudden and concealed, and the lower confining pressures and higher excess pore water pressures can make the unloading failure more destructive. Moreover, the initial unloading modulus is linearly proportional to the confining pressure but linearly inversely proportional to the excess pore water pressure.

1. Introduction

Marine sedimentary soft soils are widely distributed in coastal areas with low strength, high compressibility, high sensitivity and significant rheological engineering characteristics, which bring many technical problems to the excavation and deformation controls of soft soils foundation pit engineering. The excavation of marine sedimentary soft soils is a typical unloading project (Cai et al., 2018; Huang et al., 2019). The design calculation and numerical analysis of the soil strength parameters for those soft soils were normally obtained by axial loading tests. However, the effects of lateral unloading stress paths were ignored. Meanwhile, a high level of groundwater usually existed in the coastal areas, and the excess pore water pressure will be generated due to the construction vibration load of large construction equipment (Li, 2012). The excess pore water pressures can reduce the effective stress of soft soil particles and weaken the structure of soil particles, which can aggravate the unloading damage of soft soils. Therefore, studies on the effects of unloading stress paths and excess pore water pressures on unloading mechanical properties of soft soils are indispensable.

Previous studies were mainly focused on the strength and deformation characteristics of soft soils under the loading stress path, and those strength parameters were widely used in the design of unloading excavation and numerical simulation of soft soils. Zhang et al. (2015) used the soil parameters under loading conditions as the input of modified cambridge model to analyze the mechanical properties of the viaduct piers under unloading conditions. Ni et al. (2018) conducted a plane strain loading and unloading comparison tests in silty clay and used those strength parameters for the deformation calculation of the underground continuous wall. Above studies concluded that the numerical simulation results calculated from soil parameters under loading condition were generally smaller than actual ones.

Some researches on the unloading mechanical properties of soft soils have been reported. The stress-strain relationships of soft soils were demonstrated to be affected by the stress paths (Zeng et al., 1988; Liu and Hou, 1997). The triaxial undrained tests of soft soils in the Pearl River Delta were studied by Zhou and Chen (2009). They reported that

* Corresponding author.
E-mail address: kejun.wen@jsums.edu (K. Wen).

https://doi.org/10.1016/j.oceaneng.2019.106680
Received 3 January 2019; Received in revised form 31 August 2019; Accepted 2 November 2019
Available online 17 November 2019
0029-8018/© 2019 Published by Elsevier Ltd.

Table 1
Physical properties of soft soils.

ρ (g/cm^3)	w (%)	G_s	w_L (%)	w_P (%)	I_p	c(kPa)	ϕ (°)
1.82	39.6	2.73	41.5	25.2	16.3	19.9	28

the creep effects of soil samples under lateral unloading condition was significantly higher than that under axial loading condition. Zheng et al. (2008) conducted the unloading tests at different unloading ratios and stress paths in Tianjin silty clay. Their results indicated that the unloading ratios directly determined the magnitude and deformation of soil strain. Zhou (2013) conducted conventional triaxial shear tests and unloading direct shear tests in Guangzhou soft soils. The test results showed that the strength and initial unloading modulus of soils at unloading path were less than that at loading path respectively. Lim and Ou (2017) reported that under the undrained conditions, the unloading mechanical parameters of soft soils can accurately calculate the excavation deformations of the foundation pit. The above studies indicated that the mechanical parameters of soft soils at unloading path will better reflect the actual conditions. However, most of them used direct shear tests which failed to reflect the three-dimensional stress state of the soil samples. The triaxial test of soft soils at unloading path is still sparse. The unloading mechanical parameters of soft soils obtained from triaxial tests can be used for engineering design calculations and numerical simulation analysis of soft soil foundation pits.

In addition to being affected by the lateral unloading stress path, the unloading strength of soft soils is also strongly influenced by the excess pore water pressure (Cui et al., 2017). Zhang et al. (2004) monitored the pore water pressure at the envelope structure on the Runyang bridge and pointed out that the vibration of the external load will generate excess pore water pressure. Li et al. (2011) studied the variations of pore water pressure at clay subgrade during dynamic vibration of construction and indicated that the dissipation time of excess pore water pressure is 20–40 h. Wei et al. (2012) studied the distribution law of excess pore water pressure in soft soils caused by shield construction. Results showed that the excess pore water pressures are between 21.2 and 56.12 kPa. Wang and Sun (2004) studied the distribution law of excess pore water pressure caused by piling construction and reported that excess pore water pressures are about 43–67 kPa. The above studies have concluded that the excess pore water pressure existed in practical engineering. However, the effects of excess pore water pressure on the unloading mechanical properties of soft soils were never reported with one exception that Yan et al. (2016) studied the triaxial tensile test of soft soils. The excess pore water pressure may change the unloading mechanical parameters which are directly used for the engineering design calculation. Therefore, studies on the effect the excess pore water pressure on the unloading mechanical properties of soft soils are necessary.

The objective of this study was to investigate the effects of excess pore water pressure and unloading ratio on the unloading mechanical properties of soft soils. The data are important to providing theoretical guidance for the excavation of soft soils and can further lay the foundation for the numerical simulation analysis of soft soils unloading creep.

2. Materials and methods

2.1. Soft soils

The soils used in this study are from a foundation pit in Shenzhen, China. The sampling depth is 13.5 m. The physical properties of the soils, including density (ρ), moisture content (□), specific gravity (G_s), liquid limit (W_L), plastic limit (W_P), undrain cohesion (c), and frictional angle (ϕ), were measured and results are given in Table 1. The physical properties of soft soils were determined by ASTM standards methods including ASTM Standard D4318, ASTM D854. Meanwhile, the used soil

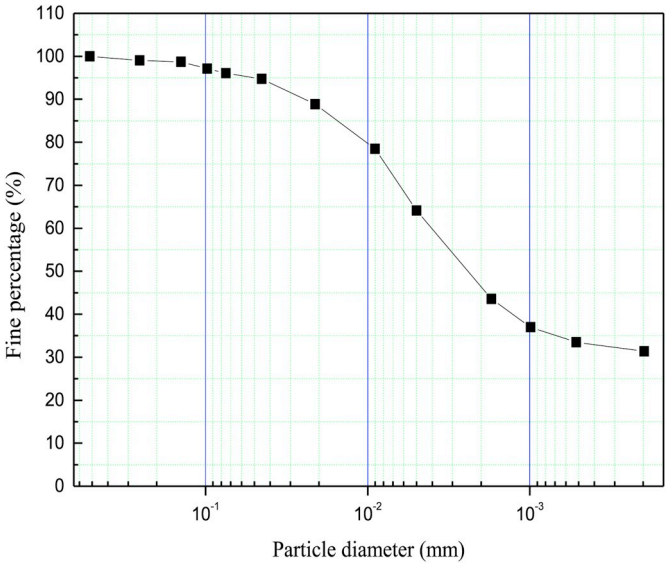

Fig. 1. Particle size distribution curve of soft soils.

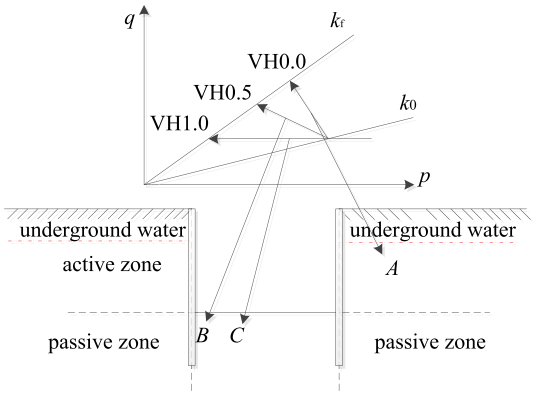

Fig. 2. Schematic diagram of excavation under soft soils.

is classified as lean clay (CL) based on USCS classification system. The oven-dried soil samples were passed through a US No.18 sieve (1 mm openings). The soil was then mixed with water to achieve 25% moisture content. The soil samples were compacted into a mold with a height of 80.0 mm and diameter of 39.1 mm through a standard compaction protocol.

The sieve analysis method was used to determining the particle composition of the selected soils, and the particle size distribution curve was shown in Fig. 1. It is clearly seen that the soft soils are mainly composed of fine particles, wherein the fine particle contents (particle size less than 0.075 mm) are 96.1%, and the clay contents (particle size less than 0.005 mm) are 64.1%.

2.2. Unloading ratios and unloading stress paths

The stress paths experienced by the soil unit in each part of the soft soil foundation pit are complicated. For the convenience of this experiment, VH*R* is used to represent different unloading stress paths, where VH represents vertical and horizontal unloading, and unloading ratio R represents the ratio of absolute value of vertical stress unloading ($|\Delta\sigma_1|$) to absolute value of horizontal stress unloading ($|\Delta\sigma_3|$), which is $R = |\Delta\sigma_1|/|\Delta\sigma_3|$.

Under the K_0 consolidation condition, the unloading compression failure occurs in the soil when the unloading ratio (R) is less or equal to 1; the unloading elongation failure happens when R is higher than 1

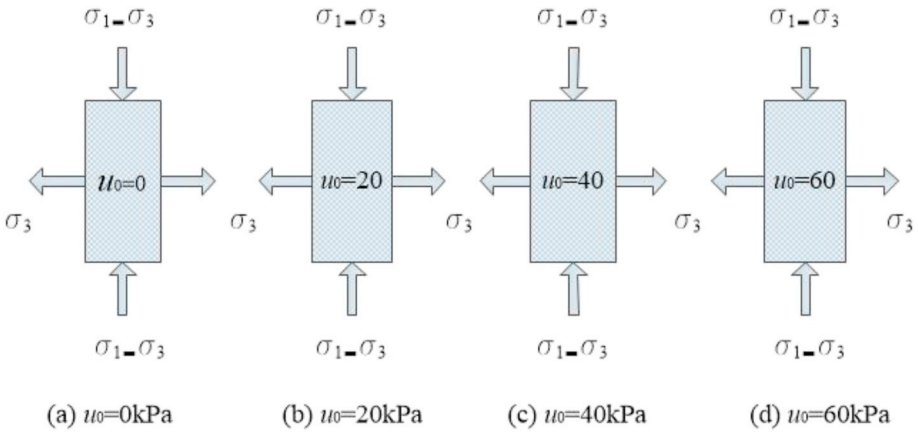

Fig. 3. Applications of excess pore water pressures.

(Zheng et al., 2008). This study mainly focused on the unloading compression failure of the selected soils, therefore, unloading ratios of 0.0, 0.5, and 1.0 were selected in this experiment. Moreover, VH0.0 corresponds to the unloading stress path experienced by point A (Fig. 2), that is, the vertical stress is constant, and the horizontal stress is gradually reduced. VH0.5 and VH1.0 correspond to the stress paths experienced by points B and C, respectively, that is, the ratio of vertical unloading and horizontal unloading are 0.5 and 1.0, respectively.

2.3. Experimental procedures

2.3.1. Saturation

The pore water pressure valve (upper drain valve) and back pressure valve (lower drain valve) of the triaxial instrument were closed firstly, and then the confining pressure (20 kPa) was applied to soil samples. The pore water pressure on the pore pressure sensor was read when the value was stable. After that, the back-pressure valve was opened to apply back pressure to the soil samples, and the confining pressure was applied in stages. After the pore water pressures were stabilized, the next level of confining pressure and back pressure were applied. The increment of each confining pressure and back pressure is 30 kPa. When the confining pressure is 110 kPa and the back pressure is 90 kPa, the Skempton's B-value calculated from each pore water pressure increment is 0.95, which indicates that soil samples are saturated. The desired saturation degree achieved after 24 h, and the used soft soils are disturbed soils with a 25% moisture content.

2.3.2. Consolidation

The three different consolidation confining pressures σ_{3c} (100, 200, and 300 kPa) were applied in this study. The corresponding axial pressures σ_{1c} (189, 377, and 566 kPa) were respectively applied to restore the sample as undisturbed state. After that, the upper drain valve of the triaxial instrument was opened to perform K_0 ($k_0 = 1 - \sin\phi' = 0.53$) drainage consolidation on the soil samples.

2.3.3. Excess pore water pressure

The excess pore water pressure (u_0) refers to the excess pore water pressure applied by the triaxial instrument back pressure system after consolidation and before the unloading tests. The excess pore water pressures were found to be 17–64 kPa in the constructions of soft soils in Shenzhen, China (Wei et al., 2012). Therefore, four different excess pore water pressures ($u_0 = 0$, 20, 40 and 60 kPa) were applied in this experiment to study the unloading mechanical properties of soft soils, as shown in Fig. 3.

2.3.4. Unloading strength tests

Soil samples were unloaded by horizontal and vertical stresses along the VH0.0, VH0.5 and VH1.0 stress paths. The detailed unloading stress path tests were summarized in Table 2. For VH0.0 unloading path, σ_1 remain same during the unloading test while σ_3 is reducing with 0.02 kPa/min unloading rate. In VH0.5 unloading path, σ_1 and σ_3 decrease with 0.01 kPa/min and 0.02 kPa/min unloading rate, respectively. For VH1.0 unloading path, σ_1 and σ_3 both decrease with a rate of 0.02 kPa/min.

2.3.5. Data collection

The axial pressures, confining pressures, axial deformations and pore water pressures were recorded until the axial strains reached 15%.

3. Results and discussion

3.1. Deviatoric stress-strain curves

Fig. 4 shows the relationships between deviatoric stress and axial strain at different confining pressures (200 and 300 kPa) and unloading ratios (0.0 and 0.5). In general, the stress-strain curves of the soil samples under unloading conditions have no essential difference compared with that under axial loading condition reported by Wang et al., (2013). When the confining pressure increases, the initial slopes of the deviatoric stress-strain curves become steeper, indicating an increase of initial unloading modulus. Meanwhile, the stress-strain curve exhibit strain hardening. This is in agreement with the results reported by Zheng et al. (2008). However, Liu and Hou (1997) found that the stress-strain curve of soft soils exhibit stain softening, which is opposite to the results in this study. This could be due to that the consolidation drainage test was conducted in their experiment. From Fig. 4(a) and (c), it can be seen that unloading ratios will affect the unloading strength of soft soils – the

Table 2
The detailed parameters of unloading tests.

Unloading stress path	Confining pressure σ_3 (kPa)	Axial pressure σ_1 (kPa)	Excess pore water pressure u_0 (kPa)
VH0.0	100	189	0,20,40,60
	200	377	0,20,40,60
	300	566	0,20,40,60
VH0.5	100	189	0,20,40,60
	200	377	0,20,40,60
	300	566	0,20,40,60
VH1.0	100	189	0,20,40,60
	200	377	0,20,40,60
	300	566	0,20,40,60

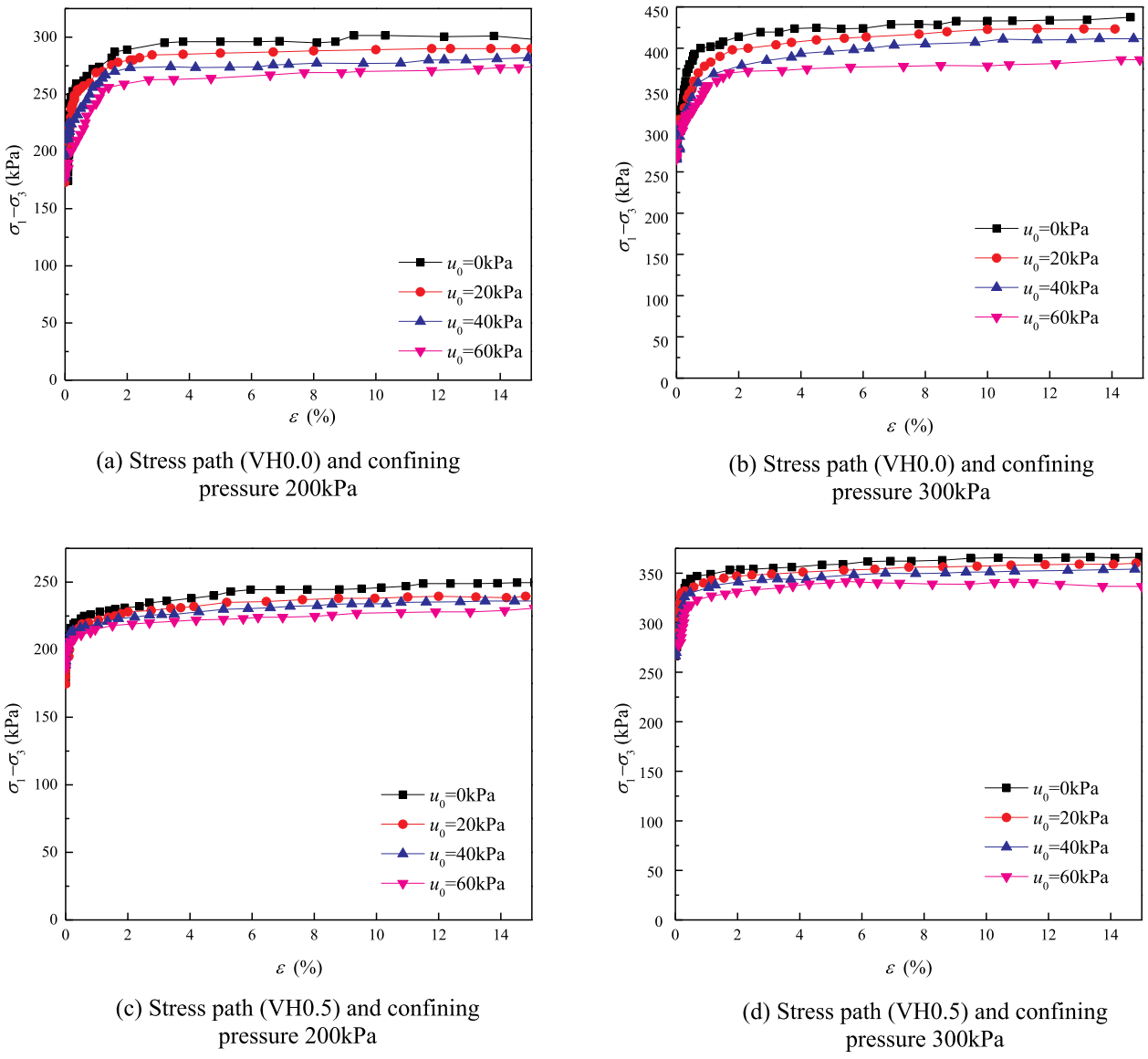

(a) Stress path (VH0.0) and confining pressure 200kPa

(b) Stress path (VH0.0) and confining pressure 300kPa

(c) Stress path (VH0.5) and confining pressure 200kPa

(d) Stress path (VH0.5) and confining pressure 300kPa

Fig. 4. Deviatoric stress-strain curves at different confining pressures (200 and 300 kPa) and unloading ratios (R = 0.0, and 0.5).

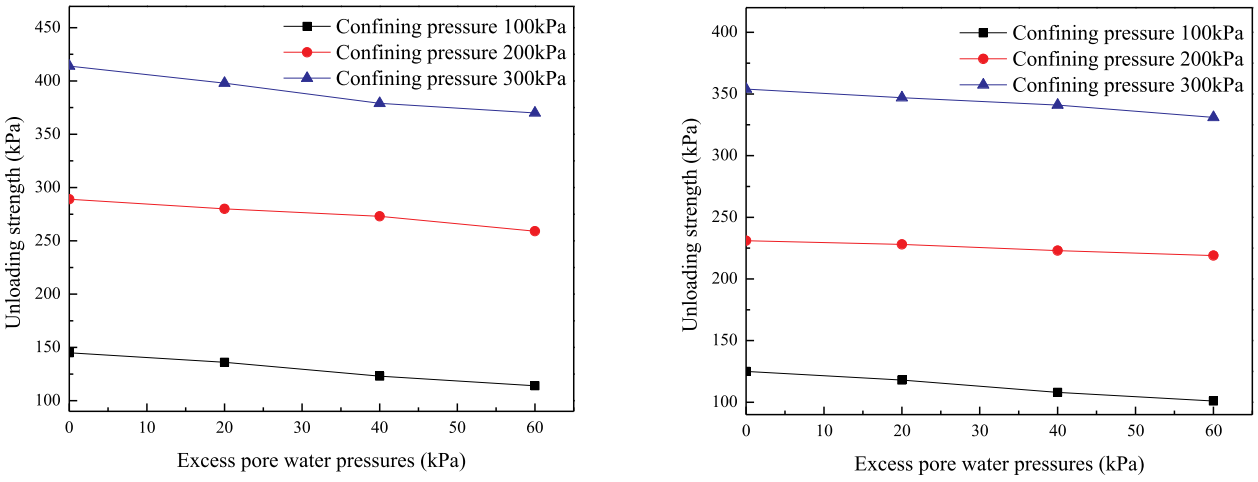

(a) Stress path VH0.0

(b) Stress path VH0.5

Fig. 5. The unloading strengths of soft soils at different confining pressures and excess pore water pressures.

Table 3
Strength parameters at different unloading stress paths.

Excess pore water pressure (kPa)	VH0.0		VH0.5		VH1.0	
	c (kPa)	ϕ (°)	c (kPa)	ϕ (°)	c (kPa)	ϕ (°)
0	33.6	33.2	28.9	34.2	14.8	35.1
20	21.4	33.0	20.5	33.6	12.8	34.2
40	11.6	31.5	9.9	33.1	9.2	33.6
60	4.0	30.8	2.9	32.3	2.5	32.5

higher unloading ratios, the lower unloading strengths. When the strain is around 1%, the corresponding deviatoric stress accounts for 70% ~83% of the unloading strength, which indicated that the axial strain is small in early stage unloading process. When the strain is 2%~3%, the strain of soft soils suddenly becomes larger and gradually increases until soil samples damage. The above phenomenon indicates that the unloading failure mode of soft soils is sudden and concealed, and the greater excess pore water pressure will cause unloading failure to be more sudden. Therefore, in the construction process of soft soil foundation pits, the deformation of the foundation pits should be closely monitored to prevent the unloading failure from happening suddenly, and the methods of reducing the groundwater level or diverting the groundwater should be used to avoid the excess pore water pressure caused by the construction vibration.

3.2. Unloading strengths

The deviatoric stress-strain curves in Fig. 4 generally do not have peaks. The deviatoric stresses keep increasing as the strains increase, indicating a strain hardening. Therefore, it is not easy to affirm the damage points. Liu and Hou (1997) pointed out that the deviatoric stress-strain curves can be expressed in double logarithmic coordinates, and the deviatoric stress-strain is in a straight-line segment with two distinct turning points. This study chooses the last turning point as the breaking point of the unloading strength. The unloading strengths of soft soils at different confining pressures and excess pore water pressures were shown in Fig. 5. It can be found that the unloading strength of soft soils decreases with increase of excess pore water pressure, indicating that the excess pore water pressure has a significant weakening effect on the unloading strength of soft soils. Comparing with the unloading strength without excess pore water pressure, the reduction rate of unloading strengths at excess pore water pressure ranging from 20 to 60 kPa were found to be 3.4%–21.4% and 1.3%–19.2% for VH0.0 and VH0.5 respectively.

The highest slope is found in the VH0.0 stress path and 100 kPa confining pressure. It is clearly seen that the slope decreases with the

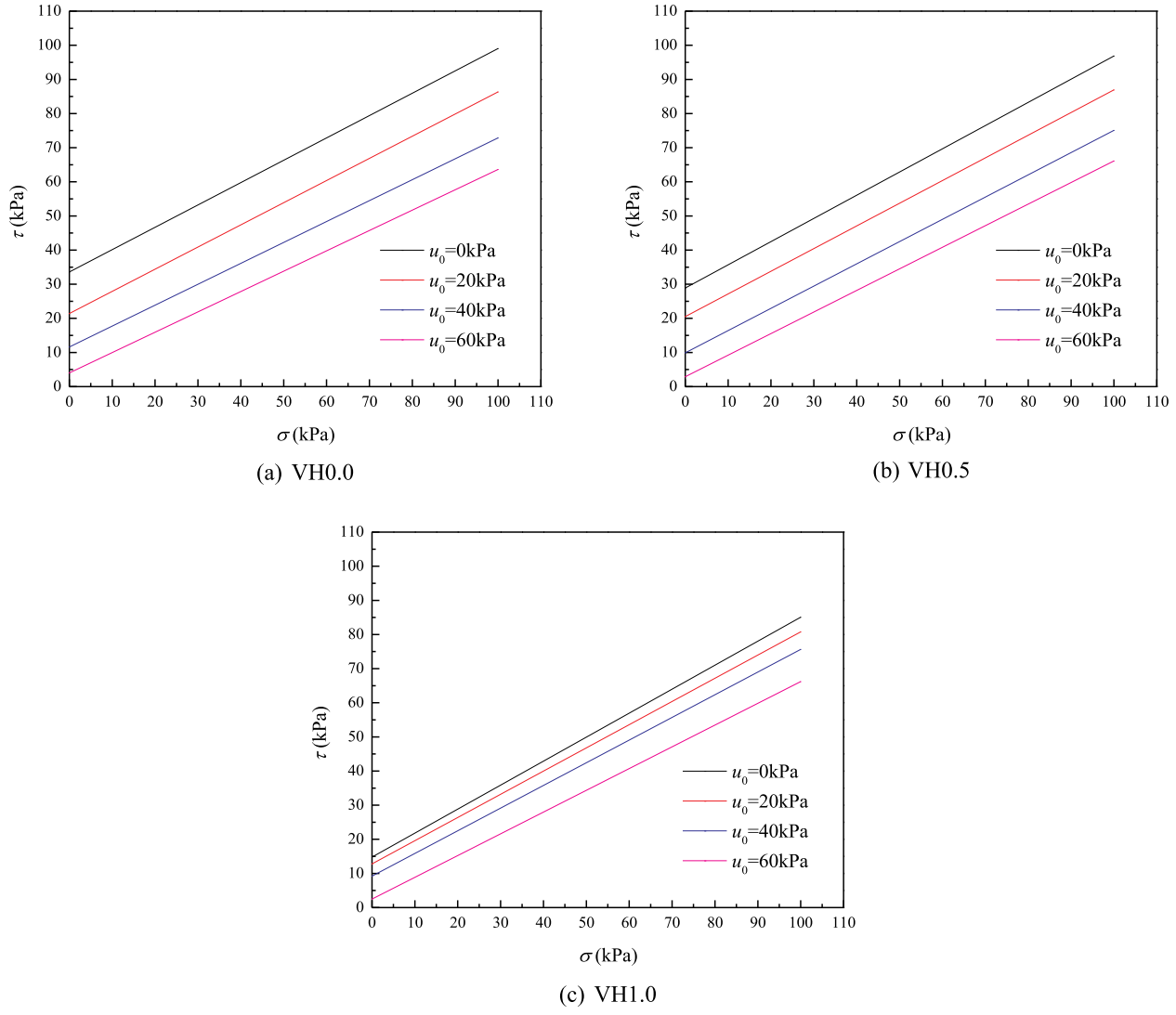

Fig. 6. Total stress intensity envelopes at different unloading stress paths.

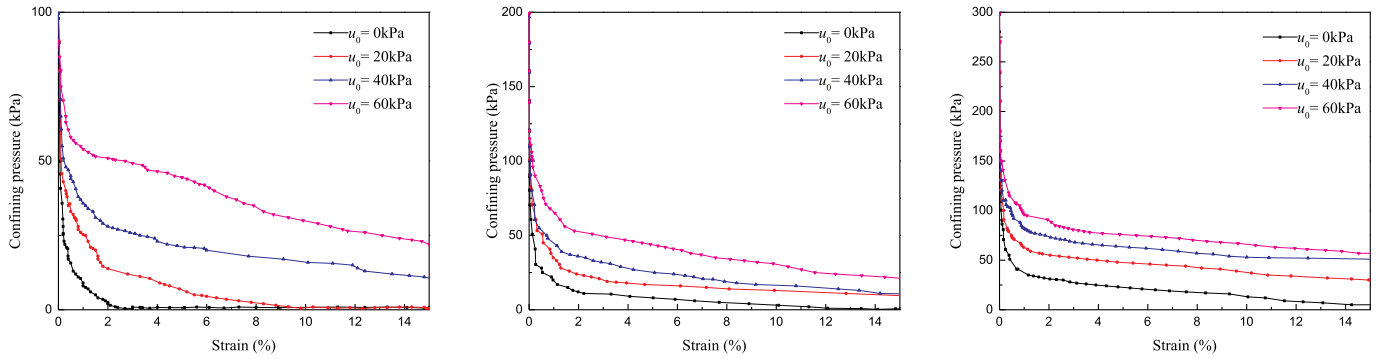

(a) Confining pressure 100kPa (b) Confining pressure 200kPa (c) Confining pressure 300kPa

Fig. 7. Confining pressure-strain curves at VH1.0 stress path at different confining pressures.

Fig. 8. Soil sample compression failure.

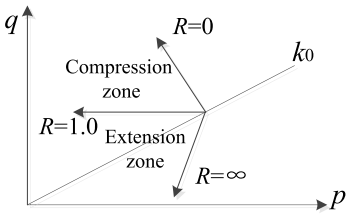

Fig. 9. Schematic diagram of the stress path at compression and extension zones.

increase of confining pressure and unloading ratio. This indicates that the unloading strength of soft soils at low confining pressure and unloading ratio decreases faster than that at higher confining pressure and unloading ratio.

3.3. Unloading strength parameters

The strength envelopes at different unloading stress path are shown in Fig. 6, and the corresponding unloading strength parameters are summarized in Table 3. It can be seen from Fig. 6 that under the same unloading stress paths, the envelopes of the total stress intensity at different excess pore water pressures are almost parallel, indicating that the internal friction angle remains constant, but the cohesion decreases as the excess pore water pressure increases. The studies by Zhuang et al. (2007) and Sun et al. (2013) on tests of silty clay also reported the similar results. Moreover, under the same excess pore water pressure,

Table 4
The initial modulus and ultimate strength of soft soils.

Stress path	σ_3 (kPa)	u_0 (kPa)	b (MPa^{-1})	E_0 (MPa)	a (kPa^{-1})	$(\sigma_1-\sigma_3)_{ult}$ [a] (kPa)	R_f [b]
VH0.0	100	0	0.079	12.642	0.012	84.034	0.99
		20	0.092	10.846	0.015	68.966	0.97
		40	0.146	6.845	0.017	60.606	0.98
		60	0.256	3.914	0.022	44.843	0.94
	200	0	0.024	42.553	0.008	123.457	0.97
		20	0.025	40.161	0.009	113.636	0.99
		40	0.031	32.258	0.010	104.167	0.99
		60	0.039	25.575	0.010	99.010	1.00
	300	0	0.014	71.429	0.006	169.492	0.99
		20	0.015	67.568	0.006	158.730	1.00
		40	0.019	53.476	0.007	149.254	0.98
		60	0.022	46.296	0.008	120.482	1.00
VH0.5	100	0	0.093	10.730	0.021	46.729	0.98
		20	0.127	7.868	0.023	42.918	0.98
		40	0.261	3.834	0.032	31.153	0.98
		60	0.413	2.421	0.046	21.930	0.95
	200	0	0.038	26.178	0.014	72.464	0.99
		20	0.040	24.876	0.016	62.500	0.99
		40	0.050	20.000	0.017	58.824	0.99
		60	0.061	16.447	0.019	51.546	0.98
	300	0	0.022	45.455	0.010	101.010	0.99
		20	0.023	43.668	0.011	93.458	0.99
		40	0.029	34.364	0.011	87.719	0.99
		60	0.033	30.120	0.013	74.627	0.89

[a] $(\sigma_1-\sigma_3)_{ult}=1/a$, ultimate strength of soft soils.
[b] $R_f=(\sigma_1-\sigma_3)/(\sigma_1-\sigma_3)_{ult}$

the cohesion of soft soils decreases with the increase of unloading ratios, but the friction angle increases slightly with the increase of unloading ratios (Table 3). This result is slightly different from the finding by Zhang et al. (2017). This could be due to that they applied consolidation drainage tests on soft soils.

3.4. Confining pressure-strain curves

The stress-strain characteristics focused on the VH0.0 and VH0.5 unloading stress paths. Since the VH1.0 stress path indicates that the vertical stress and horizontal stress are simultaneously unloaded, and the deviatoric stress always remains unchanged. Therefore, the deviatoric stress-strain curve cannot be drawn at VH1.0 stress path. The unloading characteristics of soft soils at VH1.0 stress path are analyzed by confining pressure-strain curves, as shown in Fig. 7. Under the same confining pressure, the axial strains generated by soils increase with the increase of excess pore water pressures, indicating that the excess pore water pressures have a significant weakening effect on the unloading

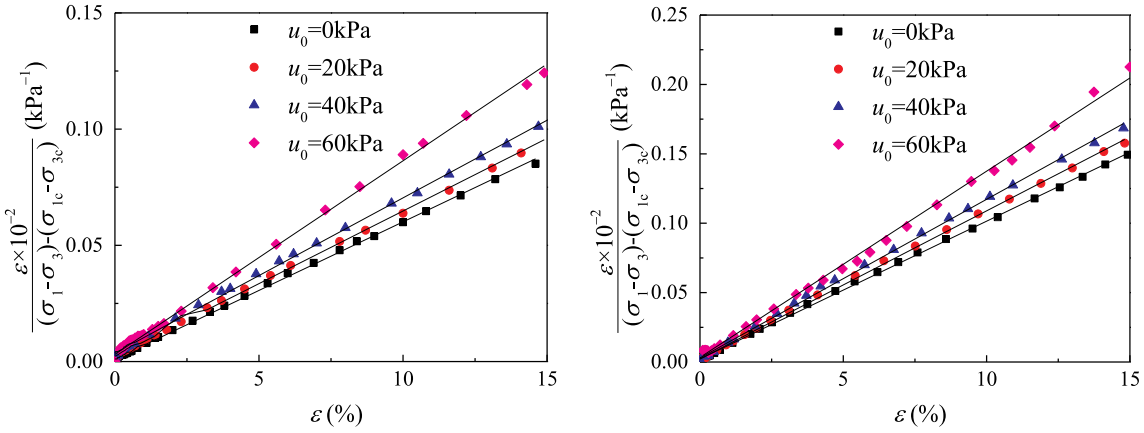

(a) VH0.0 at confining pressure 300kPa (b) VH0.5 at confining pressure 300kPa

Fig. 10. Normalization of stress-strain curves (confining pressure 300 kPa).

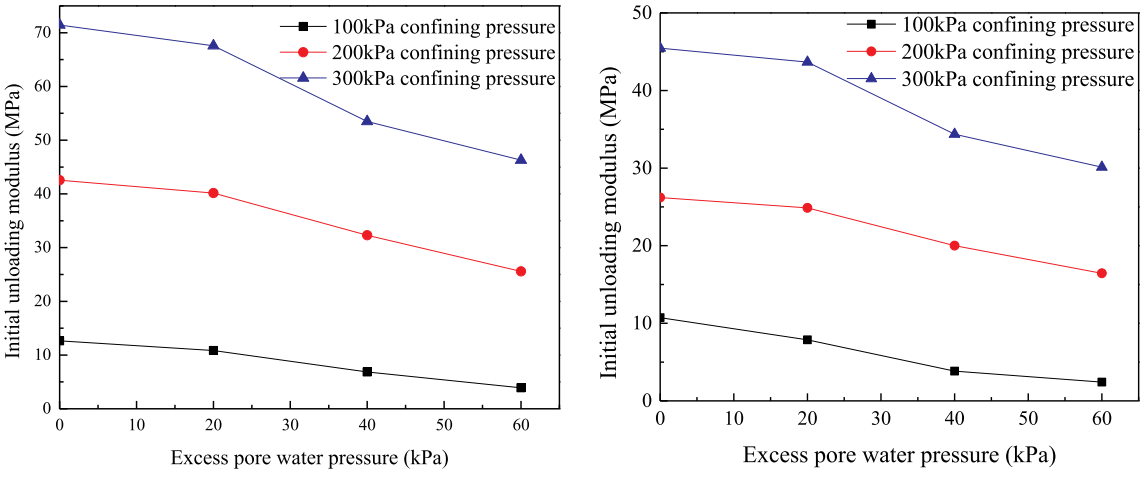

(a) VH0.0 stress path (b) VH0.5 stress path

Fig. 11. Relationship between initial unloading modulus and excess pore water pressure.

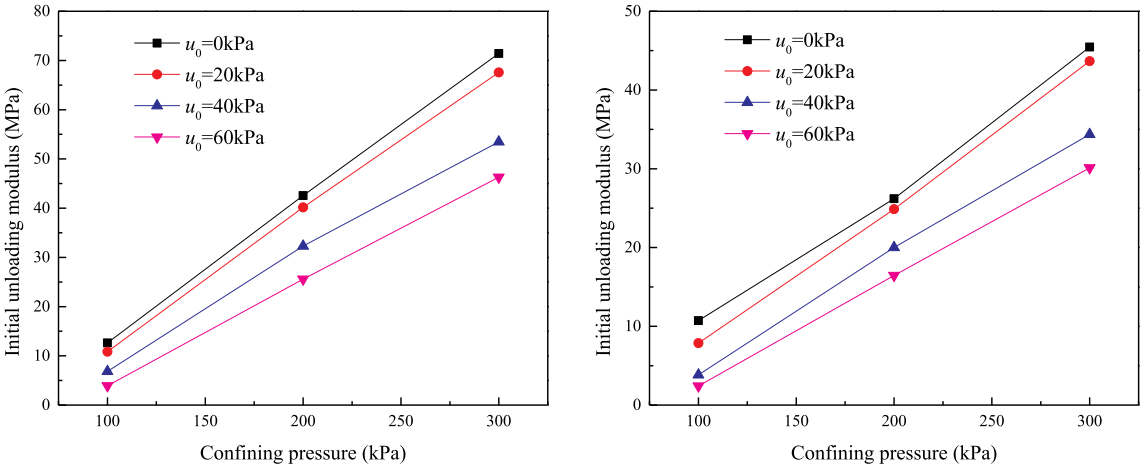

(a) VH0.0 stress path (b) VH0.5 stress path

Fig. 12. Relationships between initial unloading modulus and consolidation confining pressure.

strength of soft soils. Meanwhile, given the same excess pore water pressure, the deviatoric stresses at the unloading failure of soft soils increase with the increase of confining pressures. Therefore, increasing confining pressure of soft soils will contribute to delaying the unloading failure of soft soils.

The soil samples at VH1.0 stress path are subject to compression failure, as shown in Fig. 8. In the initial stage of unloading, the soil samples have a certain rebound displacement in the axial direction. With further process of unloading, the molar stress circles are closer to the damage envelope and the deformations of soil samples increase sharply until the shear fails. Zheng et al. (2008) conducted unloading tests at different unloading ratios (R = 0, 1, 2, 4 and ∞) in Tianjin marine sedimentary silty clay. They reported that the unloading ratio (R = 1) is the critical point between compression and extension failure of soil samples, as shown in Fig. 9. This is slightly different with our results. This could be due to that they applied isotropic consolidation on soil samples.

3.5. Analysis of initial unloading modulus

The initial unloading modulus (E_0) is an important parameter for numerical analysis of soft soil foundation pits. It is calculated by normalization of stress-strain curves of soft soils. The tangential modulus-strain relationship can be further obtained from the Equation (1) (Kondner, 1963):

$$\frac{\varepsilon}{(\sigma_1-\sigma_3)}=a\varepsilon+b \tag{1}$$

There is a linear relationship between $\varepsilon/(\sigma_1-\sigma_3)$ and strain (ε). The intercept and slope of this straight line are a and b, respectively. It can be deduced that the soil ultimate strength is 1/a, and the initial unloading modulus is 1/b. To eliminate influences of initial solidification stress difference $(\sigma_{1c}-\sigma_{3c})$ on normalization results during K_0 solidification, $(\sigma_1-\sigma_3)$ is subtracted by $(\sigma_{1c}-\sigma_{3c})$ here. Therefore, Eq. (1) can be rewritten as:

$$\frac{\varepsilon}{(\sigma_1-\sigma_3)-)\sigma_{1c}-\sigma_{3c})}=a\varepsilon+b \tag{2}$$

In the case of VH0.0 and VH0.5 stress paths, the normalized stress-strain curves at 300 kPa confining pressure are drawn according to Eq. (2), as shown in Fig. 10. It is found that all curves at different excess pore water pressures show good linear relations. This proves that Eq. (2) can normalize test results well. All parameters including, a, b, initial modulus, and soil ultimate strength, are obtained through the normalized stress-strain curve, and are summarized in Table 4.

It can be seen from Table 4 that at same unloading stress paths and confining pressures, the initial unloading modulus of soft soils decreases with the increase of excess pore water pressures. Given the same confining pressures and excess pore water pressures, the initial unloading modulus of soil samples at VH0.5 stress path is lower than that at VH0.0 stress path. This is consistent with the results in the unloading strengths. Meanwhile, it is found from Fig. 11 that the initial unloading modulus reduces slightly while the excess pore water pressure ranges from 0 to 20 kPa, but it decreases sharply as excess pore water pressure is between 20 and 40 kPa. This result suggests that the unloading failure of soil samples will happen when the excess pore water pressure ranges from 20 to 40 kPa. The certain value of excess pore water pressure needs to be further studied.

The initial unloading modulus of soil samples presents a linear growth with the increase of confining pressures, as shown in Fig. 12. Xiong et al. (2013) found the similar conclusion as excess pore water pressure is 0 kPa. The initial unloading modulus of soil samples at VH0.0 and VH0.5 stress path are 12.62 MPa and 10.75 MPa, respectively. This is similar with what Xiong et al. (2013) reported that the corresponding unloading modulus is 15 MPa while the confining pressure is 100 kPa.

4. Conclusions

A series of undrained triaxial unloading tests on marine sedimentary soft soils at different unloading ratios and excess pore water pressures were studied. The excess pore water pressure had significant weakening effects on the unloading strength parameters of soft soils, suggesting that considering excess pore water pressure in practical engineering is needed. Meanwhile, comparing with the unloading strength without excess pore water pressure, the reduction rate of unloading strengths at excess pore water pressure ranging from 20 to 60 kPa were found to be 3.4%–21.4% and 1.3%–19.2% for VH0.0 and VH0.5 respectively. Moreover, the excess pore water pressures had greater weakening degree to cohesion than to internal friction angle. The confining pressure showed a positive effect on the initial unloading modulus of soft soils, and the initial unloading modulus of soil samples at VH0.5 stress path was lower than that at VH0.0 stress path. These reported unloading strength parameters and unloading modulus in this study can be used for engineering design calculations and numerical simulation analysis of soft soil foundation pits.

Acknowledgments

This research was funded by the National Natural Science Foundation of China under Grant No. 51908097, the Scientific and Technological Research Program of Chongqing Municipal Education Commission under Grant No. KJ1713327 and No. KJ1600532, the State Scholarship Fund under Grant CSC No. 201708505131, Chongqing University of Science and Technology Research Program under Grant No. ck2017zkyb013 and ck2017zkyb010, School of Civil Engineering and Architecture under Grant No. JG201703from Chongqing University of Science and Technology, Chongqing Research Program of Basic Research and Frontier Technology by Chongqing Science and Technology Commission under Grant No. cstc2015jcyjA90012 and cstc2019jcyj-msxmX0258.

References

Cai, Y., Hao, B., Gu, C., Wang, J., Pan, L., 2018. Effect of anisotropic consolidation stress paths on the undrained shear behavior of reconstituted Wenzhou clay. Eng. Geol. 242, 23–33.

Cui, Y., Chan, D., Nouri, A., 2017. Coupling of solid deformation and pore pressure for undrained deformation—a discrete element method approach. Int. J. Numer. Anal. Methods Geomech. 41 (18), 1943–1961.

Huang, W., Wen, K., Li, D., Deng, X., Li, L., Jiang, H., Amini, F., 2019. Experiment study of lateral unloading stress path and excess pore water pressure on creep behavior of soft soil. Adv. Civ. Eng.

Kondner, R.L., 1963. Hyperbolic stress-strain response: cohesive soils. J. Soil Mech. Found. Div. 89 (1), 115–144.

Li, G.X., 2012. Static pore water pressure and excess pore water pressure—a discussion with Mr. CHEN Yu-jiong. Chin. J. Geotech. Eng. 34 (5), 957–960.

Li, X.J., Li, S.C., Yao, K., Zhu, S.C., Lv, G.R., 2011. Test study of changing rules of excess pore water pressure during dynamic consolidation at subgrade of expressway in Yellow River flood area. Rock Soil Mech. 32 (9), 2815–2820.

Lim, A., Ou, C.Y., 2017. Stress paths in deep excavations under undrained conditions and its influence on deformation analysis. Tunn. Undergr. Space Technol. 63, 118–132.

Liu, G.B., Hou, X.Y., 1997. Unloading stress-strain characteristic for soft clay. Undergr. Eng. Tunnels (2), 16–23.

Ni, P.P., Mei, G.X., Zhao, Y.L., Chen, H., 2018. Plane strain evaluation of stress paths for supported excavations under lateral loading and unloading. Soils Found. 58 (1), 146–159.
Sun, J., Hong, B.N., Liu, X., Li, J.W., 2013. Sensitivity analysis on stability of embankment slope based on cohesion and friction angle. J. Water Res. Architect. Eng. 11 (6), 99–104.
Wang, J., Guo, L., Cai, Y., Xu, C., Gu, C., 2013. Strain and pore pressure development on soft marine clay in triaxial tests with a large number of cycles. Ocean Eng. 74, 125–132.
Wang, Y.X., Sun, J., 2004. Influence of pile driving on properties of soils around pile and pore water pressure. Chin. J. Geotech. Eng. 23 (1), 153–158.
Wei, X.J., Chen, W.J., Wei, G., Hong, J., 2012. Research on distribution of initial excess pore water pressure due to shield tunnelling. Rock Soil Mech. 33 (7), 2013–2019.
Xiong, C.F., Kong, L.W., Yang, A.W., 2013. Correlation between mechanical properties of marine soft clay and stress path. Chin. J. Geotech. Eng. 35 (S2), 341–345.
Yan, S.W., Zhang, J.J., Tian, Y.H., Sun, L.Q., 2016. Pore pressure characteristics in isotropic consolidated saturated clay under unloading conditions. J. Mar. Sci. Technol. 24 (1), 19–25.
Zeng, G.X., Pan, Q.Y., Hu, Y.F., 1988. The behavior of excavation in soft clay ground. Chin. J. Geotech. Eng. 10 (3), 13–22.
Zhang, K.Y., Li, G.S., Mei, X.H., Du, W., 2017. Stress-deformation characteristics of silty soil based on K0 consolidation and drainage unloading stress path tests. Chin. J. Geotech. Eng. 39 (7), 1182–1188.
Zhang, K.Y., Zhao, Q.H., 2004. Research on the pore water pressure on the retaining structure of the deep pit. Chin. J. Geotech. Eng. 26 (1), 155–157.
Zhang, Z.X., Li, J.Y., Zhou, X., Li, W.Y., 2015. A study on the response of the piers of operating metro viaducts under the excavation-induced unloading condition. Rock Soil Mech. 36 (12), 3531–3540.
Zheng, G., Yan, Z.X., Lei, H.Y., Wang, P., 2008. Experimental studies on unloading deformation properties of silty clay of first marine layer in Tianjin urban area. Rock Soil Mech. 29 (5), 1237–1242.
Zhuang, X.S., Zhao, X., He, S.X., Zhu, R.G., 2007. An experiment study of soil mass deformability subject to true triaxial loads during unloading under drainage. Rock Soil Mech. 28 (7), 1387–1390.
Zhou, Q., 2013. J. Tests and test methods of unloading strength of soft soil. J. Yangtze River Sci. Res. Inst. 30 (3), 35–39.
Zhou, Q.J., Chen, X.P., 2009. Test research on typical mechanical characteristics of soft clay under lateral unloading condition. Chin. J. Rock Mech. Eng. 28 (11), 2215–2221.